

MHD boundary layer flow and heat transfer of micropolar fluid past a stretching sheet with second order slip

Wubshet Ibrahim¹

Received: 16 April 2015 / Accepted: 24 July 2016 / Published online: 16 August 2016
© The Brazilian Society of Mechanical Sciences and Engineering 2016

Abstract The intention of this article is to examine a second order slip flow and magnetic field on boundary layer flow of micropolar fluid past a stretching sheet. Employing appropriate similarity transformation and non-dimensional variables, the governing non-linear boundary-value problems were reduced into coupled higher order non-linear ordinary differential equation. Then, solution for velocity, microrotation and temperature has been obtained numerically. The equations were numerically solved using the function `bvp4c` from the matlab for different values of governing parameters. Numerical results have been discussed for non-dimensional velocity, temperature, microrotation, the skin friction coefficient and local Nusselt number. The results indicate that the skin friction coefficient C_f increases as the values of slip parameter γ increase. However, the local Nusselt number $-\theta'(0)$ decreases as both slip parameter γ and δ increase. A comparison with previous studies available in the literature has been done and an excellent agreement is obtained.

Keywords Second order slip flow · Micropolar · MHD · Heat transfer · Stretching sheet

List of symbols

Symbols

a Stretching constant (s^{-1})
 A, B Slip constants (m)
 B_0 Magnetic field strength ($Wb\ m^{-2}$)

C_f Skin friction coefficient
 c_p Specific heat ($J\ kg^{-1}\ K^{-1}$)
 f Dimensionless stream function
 g Dimensionless microrotation function
 j Micro-inertia density
 k Thermal conductivity of fluid ($W\ m^{-1}K^{-1}$)
 K_n Knudsen number
 $\iota = \min[\frac{1}{K_n}, 1]$
 M Magnetic parameter
 N Microrotation component normal to xy -plane (s^{-1})
 n Microrotation parameter
 Nu_x Local Nusselt number
 Pr Prandtl number
 q_w Surface heat flux ($W\ m^{-2}$)
 Re_x Local Reynolds number
 T Temperature of the fluid inside the boundary layer (K)
 T_w Temperature at the surface of the sheet (K)
 T_∞ Ambient temperature (K)
 u, v Velocity component along x - and y -direction ($m\ s^{-1}$)

Greeks

α Momentum accommodation coefficient
 β Material parameter
 γ First order slip parameter
 δ Second order slip parameter
 η Dimensionless similarity variable
 θ Dimensionless temperature
 μ Coefficient of dynamic viscosity (Pas)
 ν Coefficient kinematic viscosity of ($m^2\ s^{-1}$)
 σ Electrical conductivity
 ψ Stream function ($m^2\ s^{-1}$)
 λ The molecular mean free path (m)
 Λ Thermal diffusivity ($m^2\ s^{-1}$)
 ρ Fluid density ($kg\ m^{-3}$)

Technical Editor: Francisco Ricardo Cunha.

✉ Wubshet Ibrahim
wubshetib@yahoo.com

¹ Ambo, Ethiopia

κ	Coefficient of vortex viscosity (Pas)
Ω	Spin-gradient viscosity ($\text{m}^2 \text{s}^{-1}$)
τ_w	Wall shear stress (Pa) subscripts

Subscripts

∞	Condition at the free stream
w	Condition at the surface

1 Introduction

A large number of research papers are available in open literature which deal with the boundary layer flow of micropolar fluid past a stretching sheet due to the fact that the boundary layer flow and heat transfer of a micropolar fluid has a significant importance in engineering applications. For example, it is important in the design of chemical processing materials which are useful in polymeric liquids, foodstuffs and slurries. The pioneering work on the theory of micropolar fluid was done by Eringen [1, 2] about half a century ago. By using this theory, the mathematical model of many non-Newtonian fluids was developed for which the classical Navier–Stokes theory is inappropriate. Since then, the analysis of a micropolar fluid has got the attention of many researchers in the areas of fluid science and engineering owing to its vast applications in many modern industries. Following him, many scholars have published papers on micropolar fluid by considering different aspects under different situations. Particularly, the study of boundary layer flow of micropolar fluid past a stretching surface has received more attention than other geometrical surfaces. This is because the boundary layer flow of an incompressible micropolar over a stretching sheet has important applications in many industrial and engineering processes such as in polymer industries. Especially, the study of flow of micropolar fluids due to stretching sheet has paramount importance in many industrial and engineering applications such as liquid crystal, dilute solution of polymers and suspensions etc [3]. However, the analysis of micropolar over shrinking sheet is another aspect. Accordingly, Yacob and Ishak [4] numerically examined the boundary layer flow of a micropolar fluid past a shrinking sheet. Similarly Ishak [5] studied the effect of thermal radiation on the boundary layer flow of micropolar fluid past a stretching sheet. It was indicated that radiation reduces the heat transfer rate at the surface. Furthermore, Ishak et al. [6–8] examined MHD stagnation point flow of a micropolar fluid towards a stretching, vertical and wedge. The analysis of convection in a doubly stratified micropolar fluid was extensively studied by Sinivasacharia and RamReddy [9–11]. Their numerical result indicated that the values of microrotation changes in sign with in the boundary layer.

The study of slip flow is a classical problem, however, it is still an active research area. Many scholars have examined

slip flow under different aspects. For instance, Anderson [12, 13] examined the effects of slip, viscous dissipation, joule heating on boundary layer flow of a stretching surface. Moreover, scholars in Refs. [14–18] extended the investigation to a non-Newtonian fluid and analyzed the effects of partial slip, viscous dissipation, joule heating and MHD past a stretching surface. Furthermore, Das [19] studied the partial slip flow on MHD stagnation point flow of micropolar fluid past a shrinking sheet. The results show that an increase in slip parameter decreases the microrotation profile graphs. Still further, Noghrehabadi et al. [20] extended the study of slip flow to a nanofluid and numerically examined the effect of partial slip boundary condition on the flow and heat transfer of nanofluid past stretching sheet with prescribed constant wall temperature. Furthermore, Wubshet and Shanker [21] extended velocity slip boundary condition to thermal and concentration slip flow to a nanofluid and numerically analyzed MHD boundary layer flow and heat transfer of a nanofluid past a permeable stretching sheet with velocity, thermal and solutal slip boundary conditions.

The aforementioned studies consider only the first order slip flow. However, second order slip flow occurs in many industrial areas, but researchers have not paid much attention on it. Therefore, this study has given a full consideration to examine the effect of second order slip flow. Accordingly, Fang et al. [22] and Fang and Aziz [23] discussed viscous flow of a Newtonian fluid over a shrinking sheet with second order slip flow model. Similarly, Mahantesh et al. [24] examined second order slip flow and heat transfer over a stretching sheet with non-linear Navier boundary condition. They showed that both the first and the second order slip parameter significantly affect the shear stress. Moreover, Rosca and Pop [25, 26] investigated the second order slip flow and heat transfer over a vertical permeable stretching/shrinking sheet. The result of their study indicated that flow and heat transfer characteristics are strongly influenced by mixed convection, mass transfer and slip flow model parameters. By considering magnetic field, Turkyilmazoglu [27] studied analytically heat and mass transfer of MHD second order slip flow over a stretching sheet. Their study shows that increasing the values of magnetic parameter and second order slip parameter considerably reduce the magnitude of shear stress at the wall. Sing and Chamkha [28] also analyzed the dual solution for viscous fluid flow and heat transfer with second-order slip at linearly shrinking isothermal sheet in a quiescent medium.

To the best of author knowledge, no studies has been reported which discusses the effect of second order slip boundary condition on MHD boundary layer flow and heat transfer of micropolar fluid over a stretching sheet. Therefore, this study is targeted to fill this knowledge gap.

This study examine the effect of first, second order slip flow and magnetic parameter on boundary layer flow towards

stretching sheet in micropolar fluid. The governing boundary layer equations were transformed into a two-point boundary value problem using similarity variables and numerically solved using `bvp4c` from `matlab`. The effects of physical parameters on fluid velocity, temperature and microrotation were discussed and shown in graphs and tables as well.

2 Mathematical formulation

Consider a steady laminar boundary layer flow of a micropolar fluid past a stretching sheet with second order slip boundary condition with a constant temperature T_w . The uniform ambient temperature is given by T_∞ . It is assumed that the sheet is stretched with a velocity $u_w = ax$. Where a is a stretching constant. The flow is subjected to a constant transverse magnetic field of strength $B = B_0$ which is assumed to be applied in the positive y -direction, normal to the surface. Where T_w , T_∞ , and B_0 are temperature at the surface of the sheet, ambient temperature of the fluid and magnetic field strength respectively.

The coordinate frame selected in such away that x -axis is extending along the stretching sheet and y -axis is normal to it. The flow equations after boundary layer approximations can be defined as:

$$\frac{\partial u}{\partial x} + \frac{\partial v}{\partial y} = 0 \tag{1}$$

$$u \frac{\partial u}{\partial x} + v \frac{\partial u}{\partial y} = \frac{(\mu + \kappa)}{\rho} \left(\frac{\partial^2 u}{\partial y^2} \right) + \frac{\kappa}{\rho} \frac{\partial N}{\partial y} - \frac{\sigma B_0^2}{\rho} u \tag{2}$$

$$u \frac{\partial N}{\partial x} + v \frac{\partial N}{\partial y} = \frac{\Omega}{\rho j} \frac{\partial^2 N}{\partial y^2} - \frac{\kappa}{\rho j} \left(2N + \frac{\partial u}{\partial y} \right) \tag{3}$$

$$u \frac{\partial T}{\partial x} + v \frac{\partial T}{\partial y} = \frac{k}{\rho c_p} \left(\frac{\partial^2 T}{\partial y^2} \right) \tag{4}$$

The boundary conditions are:

$$u = u_w + U_{\text{slip}}, \quad v = 0, \quad N = -n \frac{\partial u}{\partial y}, \quad T = T_w, \quad \text{at } y = 0$$

$$u \rightarrow 0, \quad N \rightarrow 0, \quad T \rightarrow T_\infty, \quad \text{as } y \rightarrow \infty \tag{5}$$

U_{slip} is the slip velocity at the surface; Wu’s [29] slip velocity equation (valid for arbitrary Knudsen number, K_n) and used by researchers such as [17, 23, 24] is given by:

$$U_{\text{slip}} = \frac{2}{3} \left(\frac{3 - \alpha l^2}{\alpha} - \frac{3}{2} \frac{1 - l^2}{K_n} \right) \lambda \frac{\partial u}{\partial y} - \frac{1}{4} \left[l^4 + \frac{2}{K_n^2} (1 - l^2) \right] \lambda^2 \frac{\partial^2 u}{\partial y^2}$$

$$U_{\text{slip}} = A \frac{\partial u}{\partial y} + B \frac{\partial^2 u}{\partial y^2} \tag{6}$$

where A and B are constant, K_n is Knudsen number, $l = \min \left[\frac{1}{K_n}, 1 \right]$, α is the momentum accommodation coefficient with $0 \leq \alpha \leq 1$, and λ is the molecular mean free path. Based on the definition of l , it is noticed that for any given value of K_n , we have $0 \leq l \leq 1$. The molecular mean free path is always positive. Thus, it is known that $B < 0$, and hence the second term in the right hand side of Eq. (6) is a positive number. Moreover, γ is the first order velocity slip parameter with $\gamma = A \sqrt{\frac{a}{\nu}}$, which is positive, δ is the second order velocity slip parameter with $\delta = \frac{Ba}{\nu}$ is negative. x and y represent coordinate axes along the continuous surface in the direction of motion and normal to it respectively. The velocity components along x and y -axis are u and v respectively. N is the microrotation or angular velocity whose direction of rotation is normal to the x - y plane, ν is the kinematics viscosity, κ is the vortex viscosity, j is the micro-inertia density, Ω is the spin-gradient viscosity and given by $\Omega = (\mu + \frac{\kappa}{2})j = \mu(1 + \frac{\beta}{2})j$, where $\beta = \frac{\kappa}{\mu}$, T is the temperature inside the boundary layer, ρ is the fluid density, T_∞ is ambient the temperature far away from the sheet and n is microrotation parameter which is a constant such that $0 \leq n \leq 1$.

The similarity variable is defined by:

$$\eta = \sqrt{\frac{a}{\nu}} y \tag{7}$$

The dimensionless variables f, θ, g are introduced as:

$$f(\eta) = \frac{\psi}{\sqrt{avx}}, \quad g(\eta) = \frac{N}{ax\sqrt{\frac{a}{\nu}}}, \quad \theta(\eta) = \frac{T - T_\infty}{T_w - T_\infty} \tag{8}$$

The equation of continuity is satisfied if we choose a stream function $\psi(x, y)$ such that

$$u = \frac{\partial \psi}{\partial y}, \quad v = -\frac{\partial \psi}{\partial x} \tag{9}$$

Using the above similarity transformation and dimensionless variables, the governing Eqs. (1)–(4) are reduced into the ordinary differential equation as follows:

$$(1 + \beta)f''' + ff'' - f'^2 + \beta g' - Mf' = 0 \tag{10}$$

$$\left(1 + \frac{\beta}{2} \right) g'' - \beta(2g + f'') + fg' - f'g = 0 \tag{11}$$

$$\theta'' + Prf\theta' = 0 \tag{12}$$

With boundary conditions

$$f(0) = 0, f'(0) = 1 + \gamma f''(0) + \delta f'''(0),$$

$$g(0) = -nf''(0), \theta(0) = 1, \quad \text{at } \eta = 0,$$

$$f'(\infty) \rightarrow 0, \quad g(\infty) \rightarrow 0, \quad \theta(\infty) \rightarrow 0, \quad \text{as } \eta \rightarrow \infty \tag{13}$$

where the governing parameters are defined by:

$$Pr = \frac{\nu}{\Lambda}, \quad M = \frac{\sigma B_0^2}{\rho a}, \quad \beta = \frac{\kappa}{\mu}.$$

where f', θ and g are the dimensionless velocity, temperature and microrotation respectively. η is the similarity variable, the prime denotes differentiation with respect to η . γ, δ, Pr, M denotes first order slip parameter, second order slip parameter, Prandtl number and a magnetic parameter, respectively.

The engineering quantities of interest in this article are the skin friction coefficient C_f , and local Nusselt number Nu_x are defined as:

$$C_f = \frac{\tau_w}{\rho u_w^2}, \quad Nu_x = \frac{xq_w}{k(T_w - T_\infty)} \tag{14}$$

where the wall shear stress τ_w and wall heat flux q_w are given by:

$$\tau_w = \left[(\mu + \kappa) \frac{\partial u}{\partial y} + \kappa N \right]_{y=0}, \quad q_w = -k \left(\frac{\partial T}{\partial y} \right)_{y=0} \tag{15}$$

By using the above equations, we get:

$$C_f \sqrt{Re_x} = -(1 + \beta(1 - n))f''(0), \quad \frac{Nu_x}{\sqrt{Re_x}} = -\theta'(0) \tag{16}$$

where $Re_x = \frac{\rho v x}{\mu}$ and Nu_x are local Reynolds and local Nusselt numbers, respectively.

3 Numerical solution

The coupled three ordinary differential equations Eqs. (10)–(12) which are subjected to the boundary conditions Eq. (13) are solved numerically using the function `bvp4c`

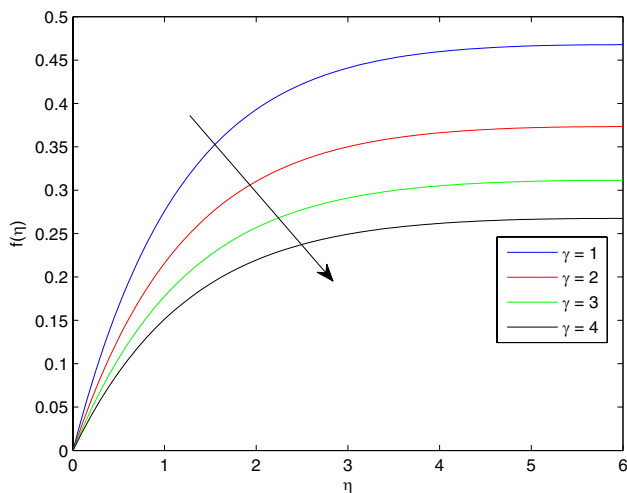


Fig. 1 Graph of f profile for different values of γ when $n = 0.5$, $Pr = M = 1, \delta = -1, \beta = 2$

from matlab for different values of physical parameters, viz. slip parameters γ and δ , Prandtl number Pr and magnetic parameter M .

4 Results and discussion

In this section, the effects of physical parameters on dimensionless velocity, temperature, microrotation, skin friction coefficient and local heat transfer rate have been discussed. Figures 1, 2 and 3 show the f profile graphs for different values of parameters such as first order slip parameter γ , second order slip parameter δ and material parameter β . The figures reveal that the boundary layer thickness increases with increasing

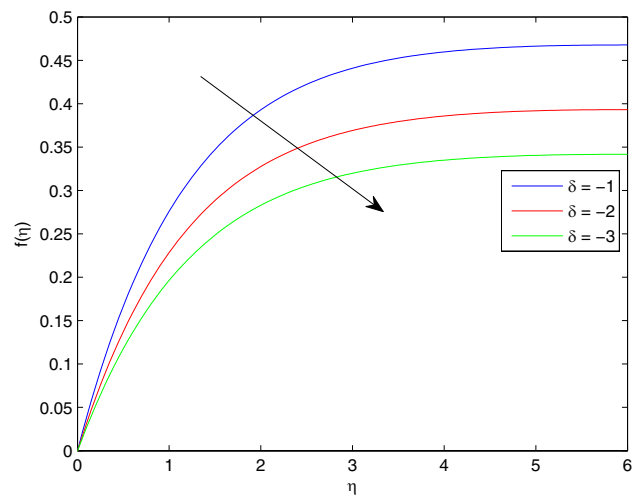


Fig. 2 Graph of f profile for different values of δ when $n = 0.5$, $Pr = M = \gamma = 1, \beta = 2$

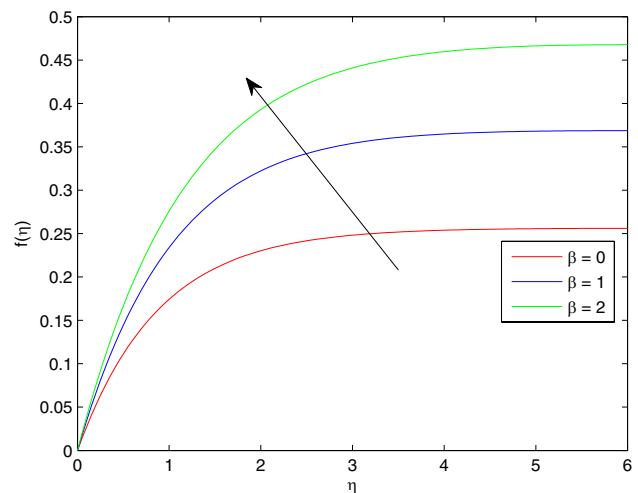


Fig. 3 Graph of f profile for different values of β when $n = 0.5$, $Pr = M = \gamma = 1, \delta = -1$

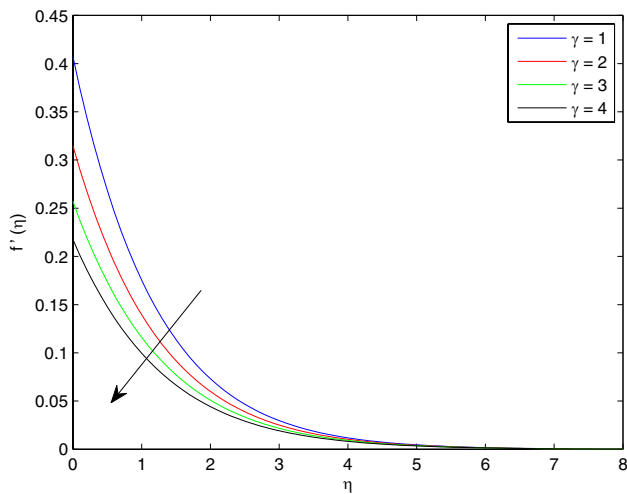


Fig. 4 Velocity profile for different values of γ when $n = 0.5$, $Pr = M = 1$, $\delta = -1$, $\beta = 2$

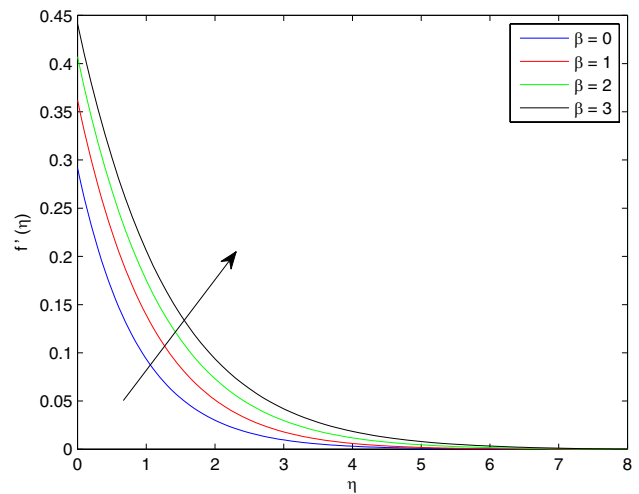


Fig. 6 Velocity graph for different values of β when $n = 0.5$, $Pr = M = \gamma = 1$, $\delta = -1$

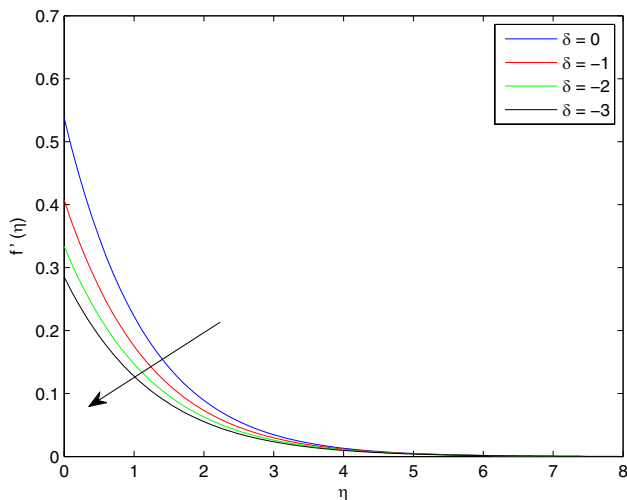


Fig. 5 Velocity profile for different values of δ when $n = 0.5$, $Pr = M = \gamma = 1$, $\beta = 2$

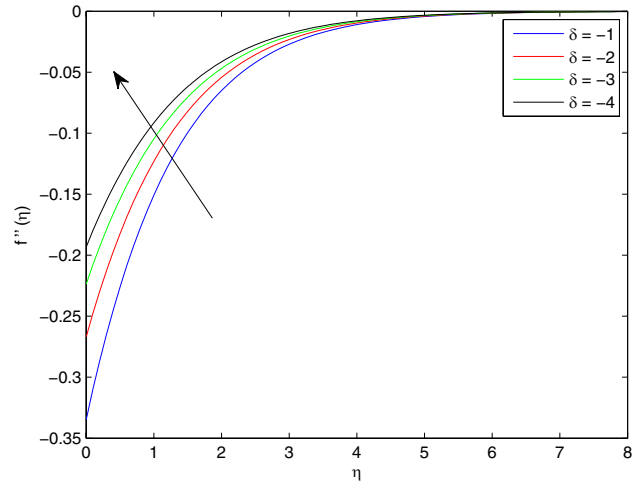


Fig. 7 $f''(\eta)$ profile for different values of δ when $n = 0.5$, $Pr = M = \gamma = 1$, $\beta = 2$

values of γ and δ while, it decreases with increasing values of β . These results are found to be in an excellent agreement with the results reported by Mahantesh et al. [24].

The non-dimensional velocity profile graph $f'(\eta)$ for various values of the first order slip parameter γ , second order slip parameter δ and material parameter β are depicted in Figs. 4, 5 and 6. These figures point out that $f'(\eta)$ is decreasing with increasing values of γ and δ , but the opposite effect is observed with β . Moreover, the velocity boundary thickness is decreasing as the values of γ and δ are increasing in absolute value and also velocity at the surface decreases as the values of γ and δ increase.

Furthermore, as the values of material parameter β increase, the surface velocity also increases.

Figures 7, 8 and 9 respectively show the effect of first order slip parameter γ , second order δ and material parameter β on the skin friction profile $f''(\eta)$. These graphs are the increasing functions of all the three parameters in absolute value. Moreover, the boundary layer thickness of the coefficient of skin friction is an decreasing function of the first and second slip parameters, but it is increasing with the material parameter β .

The effects of the slip parameters γ , δ and material parameter β , magnetic parameter M and n on temperature profile are given in Figs. 10, 11, 12, 13 and 14. From the figures, we

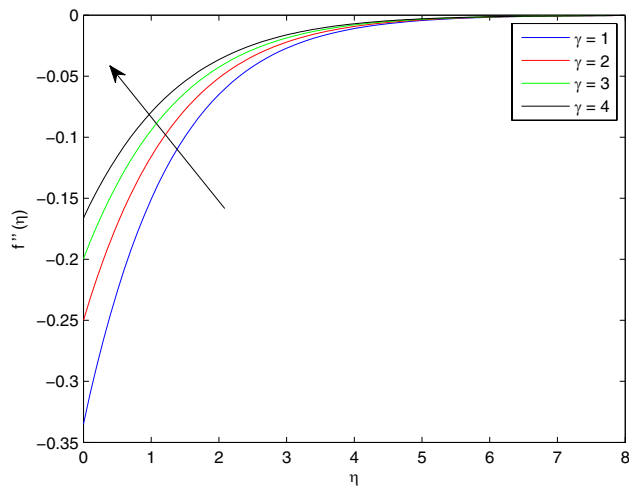


Fig. 8 $f''(\eta)$ profile for different values of γ when $n = 0.5$, $Pr = M = 1$, $\delta = -1$, $\beta = 2$

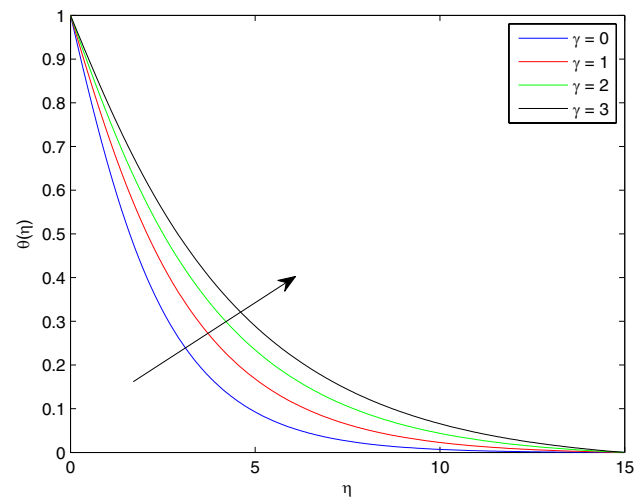


Fig. 10 Temperature profile for different values of γ when $n = 0.5$, $Pr = M = \beta = 1$, $\delta = -1$

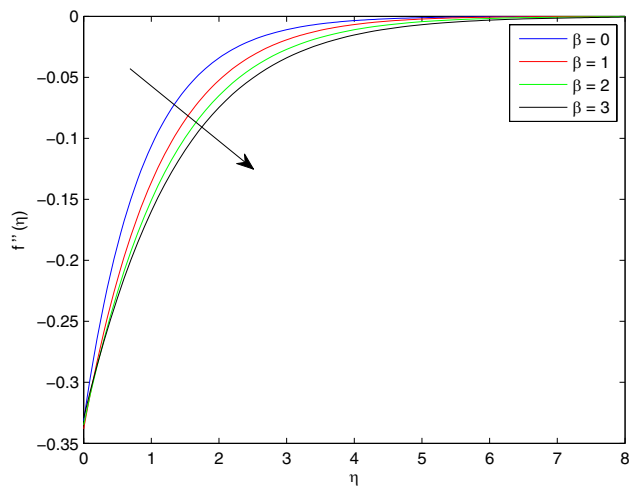


Fig. 9 $f''(\eta)$ profile for different values of β when $n = 0.5$, $Pr = M = \gamma = 1$, $\delta = -1$

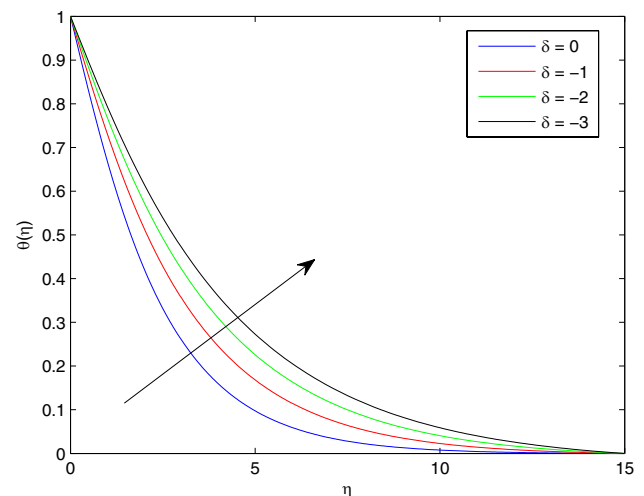


Fig. 11 Temperature profile for different values of δ when $n = 0.5$, $Pr = M = \beta = \gamma = 1$

can observe that the temperature of flow field is a decreasing function for both slip parameters. However, its thermal boundary thickness is increasing function for both slip parameters. Moreover, it is observed that the thermal boundary layer thickness is a decreasing function of material parameter β , but the thermal boundary layer thickness increases when the values of n and magnetic parameter M increase.

The microrotation (Angular velocity) profile graphs for physical parameters are given in Figs. 15, 16, 17 and 18. The graphs show that, as the values of both slip parameter γ and δ increase, the microrotation boundary layer thickness decreases. Moreover, the angular velocity at the surface decreases as both the slip parameters increase.

However, the angular velocity boundary layer thickness increases with material parameter β . Similarly, as the magnetic parameter M increases, the angular velocity boundary layer thickness decreases as shown in Fig. 18.

In order to assess the accuracy of the method used, comparison with previously reported data available in the literature has been made. From Table 1, it can be seen that the numerical values of the skin friction coefficient $-f''(0)$ in this paper for different values of γ , when $M = \delta = 0$ are in an excellent agreement with the previous results published in [14].

To further confirm the accuracy of the numerical method used in the paper, comparison of local Nusselt

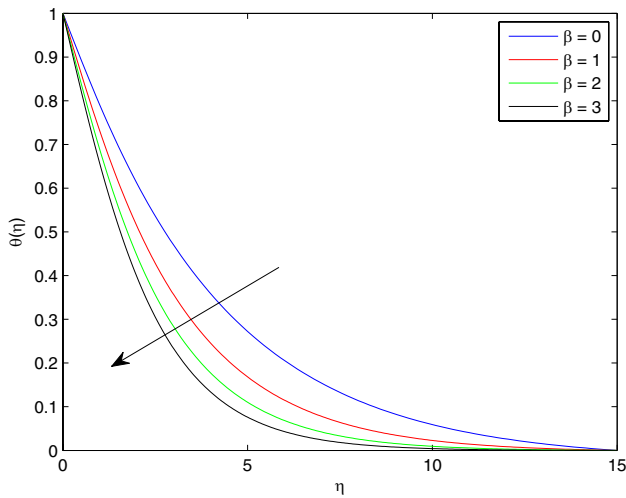


Fig. 12 Temperature profile for different values of β when $n = 0.5$, $Pr = M = \gamma = 1, \delta = -1$

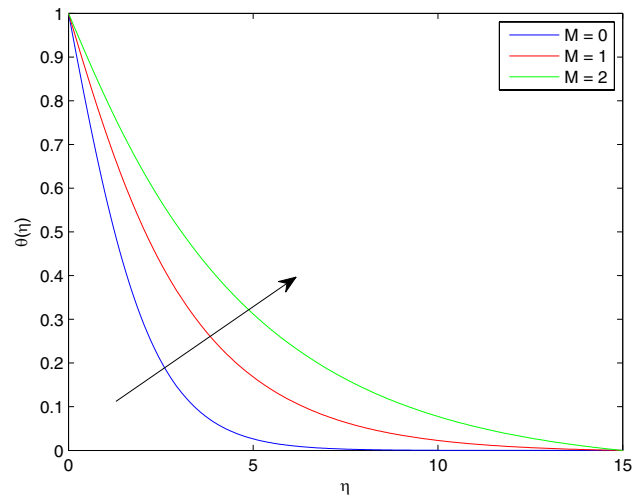


Fig. 14 Temperature graph for different values of M when $\beta = 2$, $Pr = \gamma = 1, \delta = -1, n = 0.5$

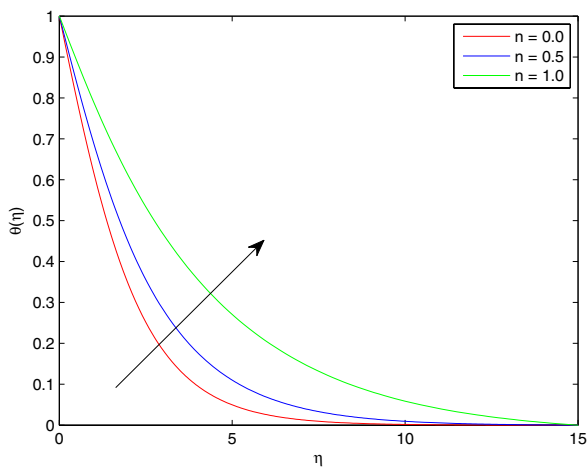


Fig. 13 Temperature graph for different values of n when $\beta = 2$, $Pr = M = \gamma = 1, \delta = -1$

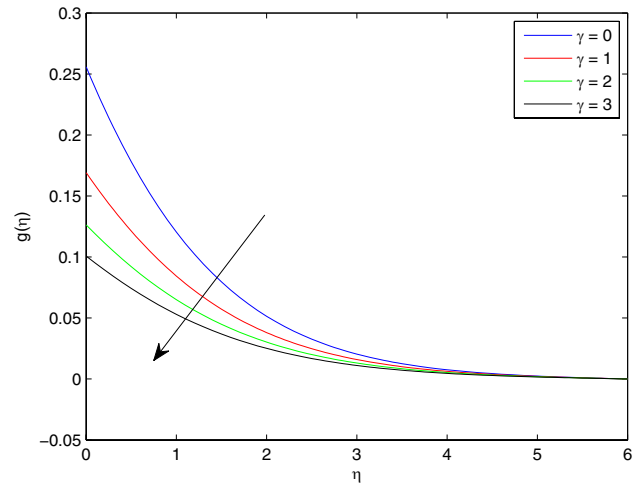


Fig. 15 Microrotation profile graph $g(\eta)$ for different values of γ when $Pr = M = \beta = 1, \delta = -1, n = 0.5$

number $-\theta'(0)$ for different values of Prandtl number Pr by ignoring the effects of M, λ and δ parameters has been shown in Table 2, which is found to be in excellent agreement with [5]. These both results indicate that the numerical used in the study is appropriate and highly accurate.

Furthermore, Table 3 shows the computed values of skin friction coefficient $-f''(0)$ and the local Nusselt number $-\theta'(0)$ for different values of the governing parameters such as M, β and δ . It is found that the heat transfer rate $-\theta'(0)$ is a decreasing function of the parameters β, γ and δ ; however, the skin friction coefficient $-f''(0)$ is an

increasing function of M , but a decreasing function of slip parameters γ and δ and material parameter β .

5 Conclusions

In this paper, the effects of second order slip flow and magnetic field on boundary layer flow and heat transfer of micropolar fluid over a stretching sheet were discussed. The boundary layer equations governing the flow problem are reduced into a couple of high order non-linear

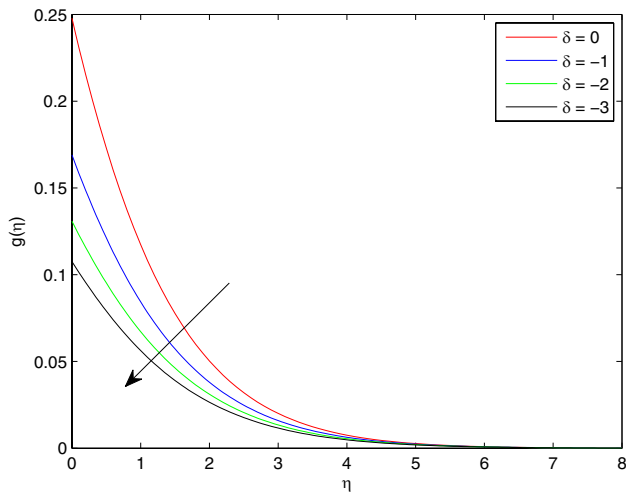


Fig. 16 Microrotation profile graph $g(\eta)$ for different values of δ when $Pr = M = \beta = \gamma = 1, n = 0.5$

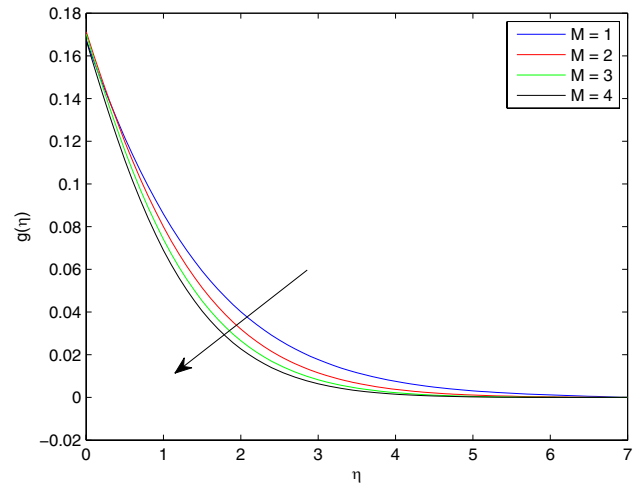


Fig. 18 Microrotation profile graph $g(\eta)$ for different values of M when $Pr = \gamma = 1, n = 0.5, \delta = -1$

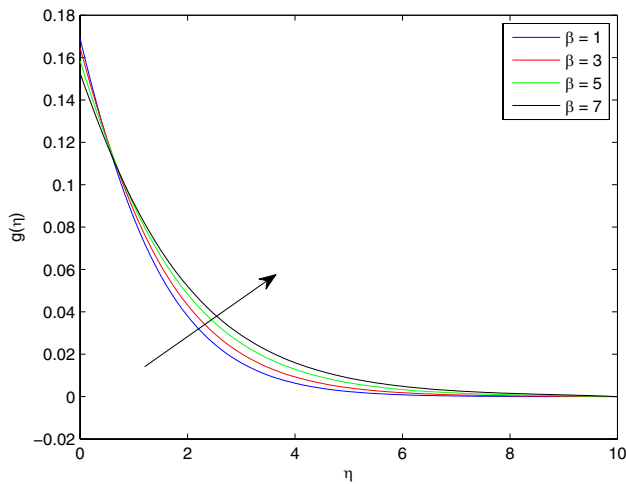


Fig. 17 Microrotation profile graph $g(\eta)$ for different values of β when $Pr = M = \gamma = 1, n = 0.5, \delta = -1$

Table 1 Comparison of values of $f''(0)$ with slip factor γ when $M = \delta = 0$

γ	Present result	Sahoo and Do [17]
0.0	1.000000	1.001154
0.1	0.872082	0.871447
0.2	0.776377	0.774933
0.3	0.701548	0.699738
0.5	0.591196	0.589195
1.0	0.430160	0.428450
2.0	0.283980	0.282893
3.0	0.214055	0.213314
5.0	0.144841	0.144430
10.0	0.081243	0.081091
20.0	0.043790	0.043748

Table 2 Comparison of local Nusselt number θ' at $\beta = M = 0.0, n = 0.5$, for different values of Pr with previously published result

Pr	Ishak [5]	Present result
0.72	0.4631	0.4636
1.0	0.5820	0.5822
3.0	1.1652	1.1652
10.0	2.3080	2.3080
100.0	7.7657	7.7657

ordinary differential equations using the similarity transformation. Then, the obtained differential equations are solved numerically using bvp4c from matlab software. The effects of various governing parameters, such as slip parameters γ and δ , magnetic parameter M , Prandtl number Pr , Material parameter β on momentum, energy and microrotation equations are discussed using figures and tables.

From the study, it is found that the flow velocity and the skin friction coefficient are strongly influenced by slip and material parameters. It is also observed that the velocity boundary layer thickness decreases as the absolute values

of slip parameters increase. However, the thermal boundary layer thickness increases as the absolute values of the two slip parameters increase. Furthermore, the skin friction

Table 3 The computed values of skin friction coefficient $f''(0)$ and local Nusselt number $\theta'(0)$ when $Pr = 1, n = 0.5$ for different values of $M\beta$ and δ

M	β	δ	$-f''(0)$			$\theta'(0)$		
			$\gamma = 1$	$\gamma = 2$	$\gamma = 3$	$\gamma = 1$	$\gamma = 2$	$\gamma = 3$
0.1	0.1	-1	0.3220	0.2399	0.1914	0.3816	0.3432	0.3167
0.2	0.1	-1	0.3262	0.2434	0.1943	0.3603	0.3214	0.2947
0.3	0.1	-1	0.3293	0.2459	0.1964	0.3411	0.3024	0.2761
0.4	0.1	-1	0.3315	0.2478	0.1979	0.3239	0.2859	0.2605
0.2	1	-1	0.3173	0.2371	0.1896	0.4066	0.3623	0.3315
0.2	2	-1	0.3068	0.2301	0.1846	0.4431	0.3954	0.3620
0.2	3	-1	0.2971	0.2239	0.1802	0.4703	0.4206	0.3856
0.2	4	-1	0.2884	0.2183	0.1763	0.4915	0.4407	0.4046
0.2	2	-1	0.3068	0.2301	0.1846	0.4431	0.3954	0.3620
0.2	2	-2	0.2588	0.2039	0.1683	0.4143	0.3767	0.3487
0.2	2	-3	0.2262	0.1841	0.1551	0.3927	0.3616	0.3375

coefficient $-f''(0)$ and the local Nusselt number $-\theta'(0)$ decrease as the absolute values of slip parameters increase.

References

- Eringen AC (1964) Simple microfluids. *Int J Eng Sci* 2:205–217
- Eringen AC (1966) Theory of micropolarfluids. *J Math Mech* 16:1–8
- Mahmoud M, Waheed S. Effects of slip and heat generation/absorption on MHD mixed convection flow of a micropolar fluid over a heated stretching surface, mathematical problems in engineering, vol 2010, Article ID 579162
- Yacob NA, Ishak A (2012) Micropolar fluid flow over a shrinking sheet. *Meccanica* 47:293–299
- Ishak A (2010) Thermal boundary layer flow over a stretching sheet in micropolar fluid with radiation effect. *Meccanica* 45:367–373
- Yacob NA, Ishak A, Pop I (2011) Melting heat transfer in boundary layer stagnation-point flow towards a stretching/shrinking sheet in a micropolar fluid. *Comput Fluids* 47:16–21
- Iskac A, Yacob NA, Pop I (2009) MHD boundary-layer flow of a micropolar fluid past a wedge with constant wall heat flux. *Commun Nonlinear Sci Numer Simul* 14:109–118
- Iskac A, Yacob NA, Pop I (2008) Magnetohydrodynamic (MHD) flow of a micropolar fluid towards a stagnation point on a vertical plate. *Comput Math Appl* 56:3188–3194
- Srinivasacharya D, RamReddy Ch. (2011) Effect of double stratification on free convection in a micropolar fluid. *J Heat Transf, ASME*, vol 133, 122502(1-7)
- Srinivasacharya D, RamReddy Ch (2011) Free convective heat and mass transfer in adoubly stratified non-Darcy micropolar fluid. *Korean J Chem Eng* 28(9):1824–1832
- Srinivasacharya D, RamReddy Ch (2010) Heat and mass transfer by natural convection in a doubly stratified non-Darcy micropolar fluid. *Int Commun Heat Mass Transf* 37:873–880
- Andersson I (2002) Slip flow past a stretching surface. *Acta Mech* 158:121–125
- Abel S, Mahesha N, Malipatil B (2011) Heat transfer due to MHD slip flow of a second-Grade liquid over a stretching sheet through a porous medium with non-uniform heat source/sink. *Chem Eng Commun* 198:191–213
- Sahoo B (2009) Effects of partial slip, viscous dissipation and joule heating on Von Karman flow and heat transfer of an electrically conducting non-Newtonian fluid. *Commun Non-linear Sci Numer Simul* 14:2982–2998
- Mahmoud A (2011) Slip velocity effect on a non-Newtonian power-law fluid over a moving permeable surface with heat generation. *Math Comput Model* 54:1228–1237
- Abel S, Kumar A, Ravikumara R (2011) MHD flow and heat transfer with effects of buoyancy, viscous and joules dissipation over a non-linear vertical stretching porous sheet with partial slip. *Engineering* 3:285–291
- Fang T, Yao S (2009) Slip MHD viscous flow over a stretching sheet—an exact solution. *Commun Non-linear Sci Numer Simul* 14:3731–3737
- Wang CY (2002) Flow due to a stretching boundary with partial slip—an exact solution of the Navier–Stokes equation. *Chem Eng Sci* 57:3745–3747
- Das K (2012) Slip effect on MHD mixed convection stagnation point flow of a micropolar fluid towards a shrinking vertical sheet. *Comput Math Appl* 63:255–267
- Noghrehabadi A, Pourrajab R, Ghalambaz M (2012) Effect of partial slip boundary condition on the flow and heat transfer of nanofluid past stretching sheet prescribed constant wall temperature. *Int J Thermal Sci* 54:253–261
- Ibrahim W, Shankar B (2013) MHD boundary layer flow and heat transfer of a nanofluid past a permeable stretching sheet with velocity, thermal and solutal slip boundary conditions. *J Comput Fluids* 75:1–10
- Fang T, Sao S, Zhang J, Aziz A (2010) Viscous flow over a shrinking sheet with second order slip flow model. *Commun Nonlinear Sci Numer Simul* 15:1831–1842
- Fang T, Aziz A (2010) Viscous flow with second order slip velocity over a stretching sheet. *Z Naturforsch A PhysSci* 65a:325–343
- Mahantesh MN, Vajravelu K, Abel MS, Siddalingappa MN (2012) Second order slip flow and heat transfer over a stretching sheet with non-linear Navier boundary condition. *Int J Thermal Sci* 58:143–150
- Rosca AV, Pop I (2013) Flow and heat transfer over a vertical permeable stretching/shrinking sheet with a second order slip. *Int J Heat Mass Transf* 60:355–364
- Rosca NC, Pop I (2013) Mixed convection stagnation point flow past a vertical flat plate with a second order slip: heat flux case. *Int J Heat Mass Transf* 65:102–109
- Turkyilmazoglu M (2013) Heat and mass transfer of MHD second order slip flow. *Comput Fluids* 71:426–434
- Singh G, Chamkha AJ (2013) Dual solutions for second-order slip flow and heat transfer on a vertical permeable shrinking sheet. *Ain Shams Eng J* 4:911–917
- Lin W (2008) A slip model for rarefied gas flows at arbitrary Knudsen number. *Appl Phys Lett* 93:253